

STRUCTURE AND STRENGTH CAST HIGH ALUMINUM AND MANGANESE OF IRON ALLOYS WITH A HIGH CARBON CONTENT

Bronz A., Deminskaya V., Kaputkina L., Kindop V., Kremyansky D.,
Prokoshkina V., Svyazhin A., Siwka J.
National University of Science and Technology «MISIS», Moscow, Russia

Abstract: Metallographic methods, X-ray diffraction and magnetometric analysis, hardness measurement, analysis diagrams of phase-rule diagrams and hot compression tests were used for the investigation of the Fe + (12,7 – 25,6)% Mn + (0 – 14,4)% Al + (0,02 – 2,18)% C + (0,001 – 0,135)% N alloys structure and properties and for the assessment of the as-cast alloys strength and deformability.

KEYWORDS: AS-CAST HIGH-MANGANESE-ALUMINUM IRON ALLOYS, PHASE-RULE DIAGRAMS, HOT DEFORMATION, MICROALLOYING WITH NITROGEN, E-MARTENSITE.

1. Introduction. High-strength alloys based on Fe-Mn-Al-C represent a new group of high-manganese alloys with high aluminum content (so-called TRIPLEX alloys). At the initial stage the creation of the investigated alloys, containing (12,7 – 25,6)% Mn, Al (up to 14,4)%, carbon and carbon or nitrogen, was mainly motivated by the opportunity to replace the more expensive austenitic chromium-nickel corrosion-resistant steel, which coincide with the investigated alloys in many aspects of using.

However the choice of a new complex alloying of high-manganese alloys containing aluminum, carbon and nitrogen, so a new set of realizable properties in the alloys, of course, gives new possibilities for their application. These alloys have high ductility combined with high specific strength and are very popular in terms of their use in the automotive industry [1].

Moreover the high-aluminum manganese alloys in heat-treated condition are nonmagnetic (or low magnetic) and lighter than traditional high-strength structural steels by 10 – 20%, which makes possible their use in the high frequency electrical equipment as a material for high-strength lightweight rotating parts due to their low specific weight.

In addition, these alloys are promising to use in cryogenic engineering for transportation and storage of liquefied gases [2].

It is known from the literature data [3,4] and the works of authors [2, 5-7] ϵ -martensite can be formed in the high-manganese alloys structure which maximum quantity is observed at density of manganese about 17 % mass. The characteristic feature of high-aluminum manganese alloys with high content of carbon is the presence in the structure of k-carbide variable composition (Fe,Mn)₃AlC_{1-x} with FCC lattice in which atoms of iron or manganese are arranged on the faces, and a carbon atom is in the center.

At the present time in the world there are more of projects, which examine the reactions and processes of structure formation

in the above-mentioned types of alloys for better regulation of the achieved properties, taking into account the complexity of production, especially the high-alloy steels [2, 5-8].

Thanks to introduction of nitrogen in steel the expected life of products increases, necessary level of constructional properties is provided. It surpasses many other alloying elements in hardening ability and on corrosion stability increase [9-11]. Nitrogen use in a role of alloying constituent and taking into account economic efficiency is expedient. Therefore, the aim of present study was to investigate the influence on the structure and properties of Fe-Mn-Al-C microalloying with nitrogen alloys, considering that the nitrogen is almost always present in steel in small quantities.

2. Materials and experimental procedure. The chemical composition of the alloys is shown in Table 1.

Melting of № 1 – 13 alloys was carried out in a laboratory resistance furnace with a tungsten heater at a temperature of 1600 °C by the method of net charge components fusion (carbonyl iron + ferromanganese + technical pure aluminum). Alloys samples № 1 – 13 were cylinders with 5.0 – 7,0 mm diameter. Alloys № 14, 15 and 16 are derived from net charge (metal carbonyl iron + manganese + technical pure aluminum) by flash smelting in an argon atmosphere at a P_{Ar} = 0,9 MPa pressure. The ingots were in the form of a truncated cone with maximum 3 mm cross-section and 12 mm length.

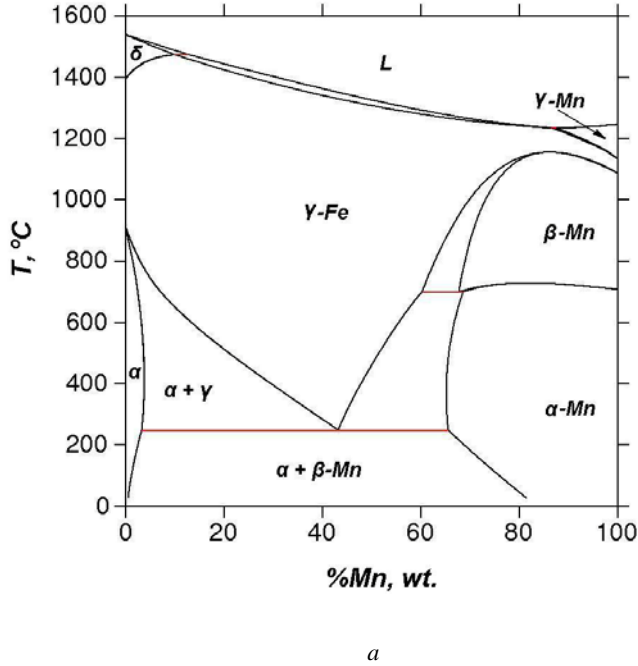
The phase-rule diagrams calculated by Thermo-Calc program were analyzing. The vertical lines on the polythermal sections of the calculated diagrams correspond to the investigated alloys specific chemical compositions. Experimentally the Fe-Mn-Al-C(-N) structure, phase composition, their magnetization were studied by the methods of metallographic, magnetometric and x-ray diffraction analysis, hardness measurement. The Fe-Mn-Al-C(-N) alloys were dipped in phosphoric acid with chromic anhydride, and Fe-Mn-Al alloys – in 3% spirit a nitric acid solute.

Table 1 - Chemical composition of the alloys.

Alloy №	Mass fraction of element, wt. %					
	Mn	Al	Si	Mo	C	N
1	16,8	0,01	0,86	2,0	1,62	0,020
2	21,2	6,2	0,50	0,20	1,10	0,006
3	19,1	7,5	0,60	1,20	1,47	0,002
4	19,1	9,0	0,50	0,03	2,18	0,001
5	23,9	4,0	0,54	0,01	1,80	0,032
6	25,3	0,01	0,20	<0,001	0,02	0,014
7	23,7	7,5	0,20	<0,001	0,05	0,008
8	22,6	14,4	0,20	<0,001	0,05	0,007
9	23,8	4,6	0,20	<0,001	0,05	0,020
10	25,6	0,01	0,20	<0,001	0,03	0,135
11	23,7	8,1	0,20	<0,001	0,05	0,008
12	24,3	11,5	0,20	<0,001	0,03	0,045
13	24,1	5,3	0,32	<0,001	0,04	0,024
14	13,4	7,5	–	–	–	–
15	12,7	7,5	–	–	–	–
16	14,0	12,0	–	–	–	–

The strength and deformability of the as-cast alloys were assessed by hot compression tests of cylindrical samples of height $h = 9,70 - 11,45$ mm and diameter $\varnothing = 5,50 - 6,20$ mm, hot deformation diagrams obtained in compression along the axis of cylindrical samples at a temperature $T = 1000$ °C with a strain rate $\dot{\epsilon} = 0,1$ s⁻¹ using the test facility «Gleeble System 3800».

3. Results and discussion. The phase-rule diagrams analysis allows predicting the following. Binary alloys of Fe-Mn with a high content of manganese are prone to phase separation in the liquid phase during cooling of the melt until the composition corresponding to the β -Mn formation and regions with a relatively low concentration of manganese (Fig. 1,a). During their rapid cooling in Fe-Mn alloys $\gamma \rightarrow \epsilon$ transformation takes place and the paramagnetic ϵ -martensite formation with the HCP shear mechanism of the martensitic type lattice. As a result of as-cast alloy with a high content of manganese may have a three-phase structure of the $\gamma + \epsilon + \beta$ -Mn.



After rapid cooling nonaluminum alloy Fe + 13,5% Mn (Fig. 1,b) is purely austenitic, as an effective γ -manganese stabilizer. In the process of doping with aluminum, which, in contrast, is a strong α -stabilizer, γ -region of the solid solution becomes narrower. The alloys (Fe+13,5% Mn) - Al become a pure ferrite with more than 5% Al. Then the investigated alloys № 14, 15 and 16 correspond to a single-phase α -region at the fast cooling and crystallization of alloys.

Phase-rule diagram polythermal sections (Fe+23,5% Mn) - Al alloys, № 6 - 13 of the Fe-Mn-Al(N) system and (Fe+19,1%Mn+9,0%Al+0,50%Si+0,03%Mo) - C, alloy №4 are shown in Figure 2.

Alloying of aluminum reduces the bundle, extends the existence of α -phase, inhibits the $\gamma \rightarrow \epsilon$ transformation, as a result the α -phase, or the α -phase with a small amount of austenite and ϵ -martensite may be in the indicated range of Mn and Al concentration in the structure of ternary alloys.

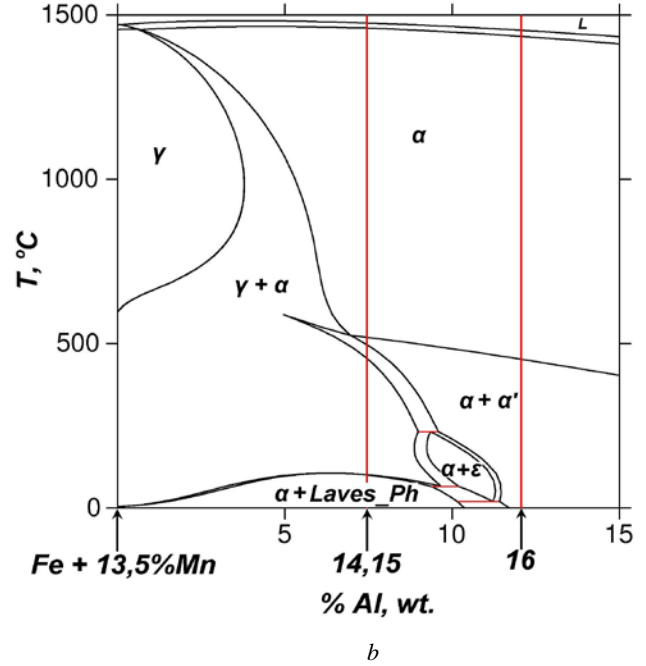
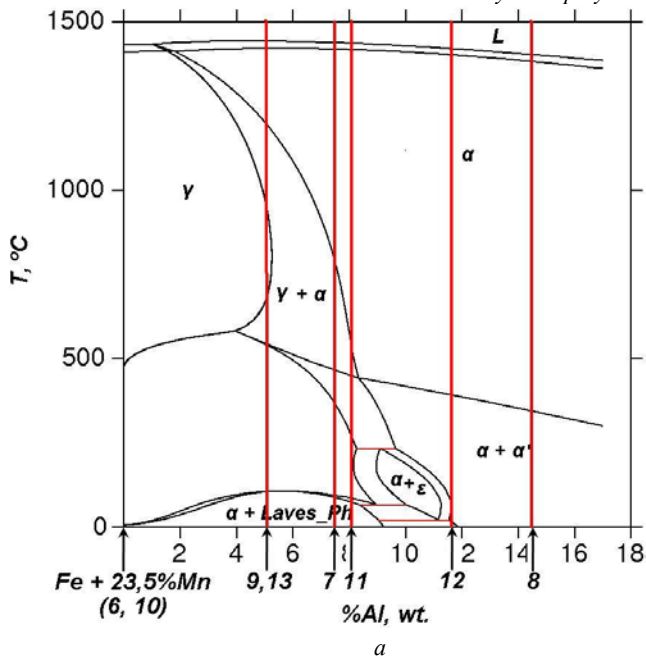
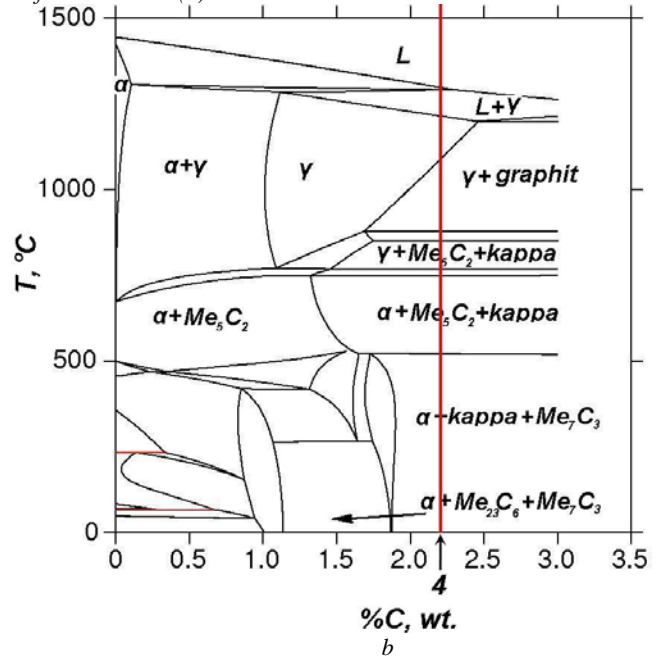


Figure 1 – The phase-rule diagrams of Fe-Mn (a) alloys and polythermal sections for № 14 – 16 (b)



The polythermal sections (Fe + 23,5% Mn) - Al



The polythermal sections

(Fe + 19,1%Mn + 9,0%Al + 0,50%Si + 0,03%Mo) - C

Figure 2 – The polythermal sections of the phase-rule diagrams (Fe + 23,5% Mn) - Al alloys, № 6 - 13 (a) and (Fe + 19,1%Mn + 9,0%Al + 0,50%Si + 0,03%Mo) - C, alloy №4 (b)

Microalloying with nitrogen also aids to reduce the separation of the melt austenite stabilization to lower the martensitic transformation temperature and reduce the number of ϵ -martensite formed during cooling. At higher nitrogen (up to 0,135%) content aluminum nitride appears in the diagram, and the gas phase, the passage through this phase of the alloy can lead to the appearance of pores during the crystallization and discontinuities in the cast material.

Alloying of Fe-Mn-Al alloys with carbon or carbon and nitrogen complicates the form of the phase-rule diagrams and as a result the phase composition of these alloys at room temperature will contain γ or γ +carbides.

Analyzing the calculated phase-rule diagrams, one should bear in mind that they are true only for equilibrium crystallization at infinitely slow cooling rates.

Experimental researches have shown that high-carbon alloys in cast state have a dendritic structure (Fig. 3a). Alloy samples of ternary system Fe-Mn-Al 14 – 16 have a grain structure (Fig. 3b) with a grain size of 40 – 50 μm .

The experimental results of X-ray phase analysis well agree with forecast, proceeding from the calculated phase-rule diagrams and crystallization and cooling conditions. The phase compositions of the as-cast alloys calculated by Thermo-Calc and obtained by means of X-ray investigation are shown in Table 2.

In addition as a result of X-ray analysis of the solid solutions lattice parameters is shown that the condition of each alloying components contributions additivity, which are proportional to their concentration, the change in the lattice period γ -and α -phases are

not applicable for alloys containing more than 3% aluminum. The difference between the experimentally obtained lattice constants of the alloy 4, containing 9% Al and nonaluminum alloy 1 is $\Delta a_{\gamma \text{ exp.}} = 0,0841 \text{ \AA}$ (for $\Delta \text{Mn} = 2,3\%$, $\Delta \text{Al} = 8,9\%$, $\Delta \text{C} = 0,56\%$, $\Delta \text{Mo} = 1,97\%$, $\Delta \text{N} = 0,019\%$), it is considerably greater than the difference of the lattice parameters, calculated using the reference values of the aluminum lattice dilatation coefficient ($\Delta a_{\gamma \text{ th.}} = 0,0285 \text{ \AA}$), based on the difference in chemical composition alloys 1 and 4. For the alloy 5 containing 4,0% Al, the difference (compared with the nonaluminum alloy 1) between the experimentally obtained and theoretically calculated lattice periods γ -phase is not so great as in the previous case, and consists $\Delta a_{\gamma \text{ exp.}} = 0,0325 \text{ \AA}$, and $\Delta a_{\gamma \text{ th.}} = 0,03518 \text{ \AA}$, respectively.

Crystallization of high Fe-Mn-Al-C-N alloys passes the formation of dendritic structures even at cooling rates of $10^3 - 10^4 \text{ K/s}$, preservation nonequilibrium high-temperature phases after cooling and separation of carbides. The released carbides resistant to dissolution by heating to 1070 – 1090 $^{\circ}\text{C}$. The hardness of alloys in the cast state is shown in Figure 4.

The high-carbon cast Fe-Mn-Al-C alloys are well hot deformed up to 40 - 50% reduction without hot cracks formation. The resistance to hot deformation σ_{max} increases with increasing content of aluminum, carbon and nitrogen. In the hot deformation diagrams (fig. 5) of alloys doped with aluminum some characteristics are observed, possibly they associate with phase changes (aging and $\gamma \rightarrow \alpha$ transformation).

The resistance of hot deformation for the alloys № 1 – 5 at $T=1000 \text{ }^{\circ}\text{C}$, $\dot{\epsilon}=0,1 \text{ sec}^{-1}$ are shown in Table 3.

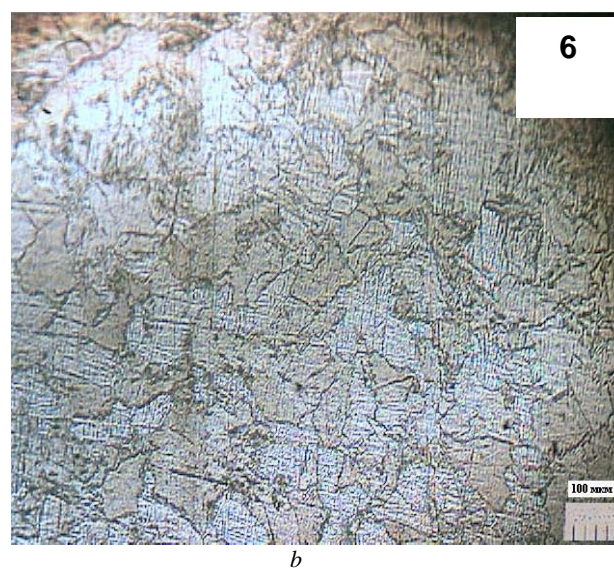
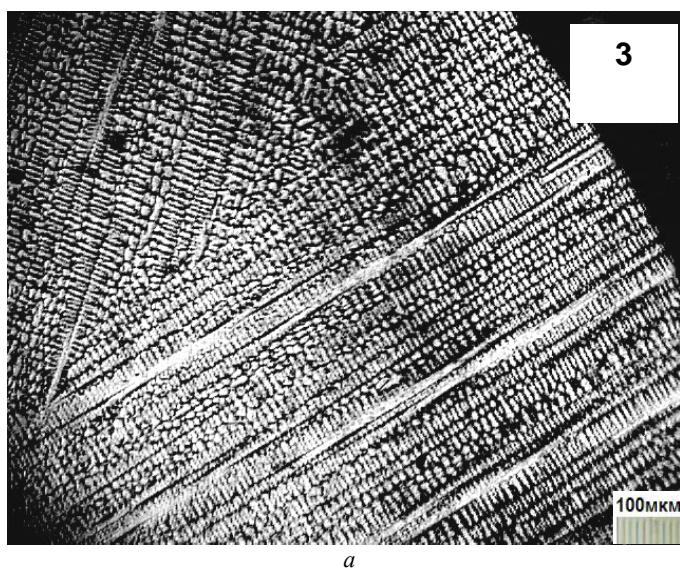


Figure 3 – The microstructure of alloys 3 (a) and 6 (b) in the cast state. The cross-sections of ingots

Table 2 – The phase compositions the as-cast alloys calculated by Thermo-Calc and obtained by means of X-ray investigation

Alloy, №	The phase compositions calculated by Thermo-Calc at 25 $^{\circ}\text{C}$	The phase compositions by means of X-ray investigation at 25 $^{\circ}\text{C}$
1	$\gamma + \text{Fe}_3\text{C} + \text{Me}_x\text{C}_y$	$\gamma + \epsilon$ (следы)
2	$\alpha + \gamma + \text{Me}_x\text{C}_y$	$\gamma + \text{кappa}$ (следы)
3	$\alpha + \text{Me}_x\text{C}_y$ (+kappa)	γ
4	$\alpha + \text{Me}_x\text{C}_y + \text{kappa}$	$\gamma + \text{kappa}$
5	$\alpha + \text{AlN} + \text{Me}_x\text{C}_y$ (+kappa)	γ
6	$\gamma + \alpha$ (+ ϵ)	$\gamma + \epsilon + \beta\text{-Mn}$
7	α (+ γ)	α
8	α	$\alpha + \epsilon$
9	$\alpha + \gamma$	$\gamma + \epsilon$ (следы)
10	$\gamma + \alpha$ (+ ϵ)	$\gamma + \epsilon + \beta\text{-Mn}$
11	α (+ γ)	$\alpha + \epsilon$
12	α	$\alpha + \gamma$ (следы)
13	$\alpha + \gamma$	γ
14	α	α
15	α	α
16	α	α

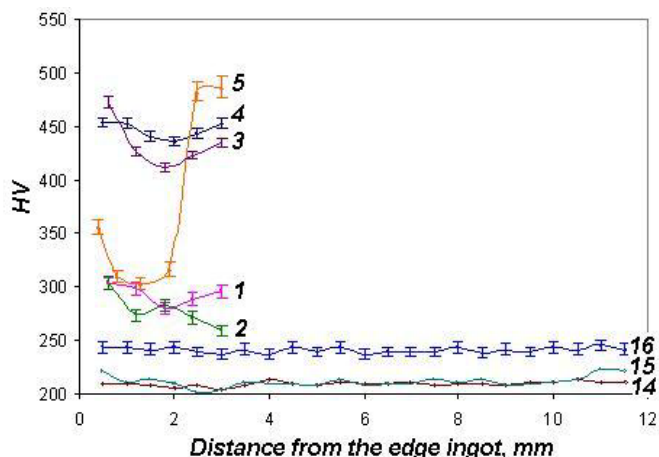


Figure 4 – The hardness of high Fe-Mn-Al-C-N cast alloys

After hot deformation and quenching the cross section hardness of all samples is aligned with the exception of alloy 4 (Fig. 6). The reasons of inhomogeneity can be its severe cracking during rapid cooling and open barrel shape. The hardness levels of samples 4 and 5, 1 in as-cast and deformed state are similar, the hardness of sample 2 after hot deformation and rapid cooling is much higher. For sample 3, conversely, it is lower than in the cast state, which is probably due to the different phase transformations occurring during crystallization cooling, strain, deformation and final cooling.

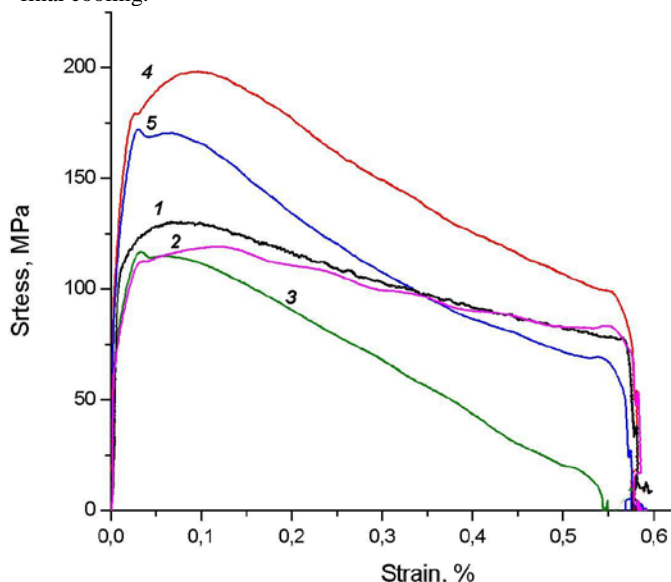


Figure 5 – Hot deformation diagrams of alloys 1 – 5. $T=1000\text{ }^{\circ}\text{C}$, $\dot{\epsilon}=0,1\text{ s}^{-1}$

Table 3 – The resistance of hot deformation for the alloys № 1 – 5 at $T=1000\text{ }^{\circ}\text{C}$, $\dot{\epsilon}=0,1\text{ sec}^{-1}$.

	Alloy №				
	1	2	3	4	5
$\sigma_{\max}^{1000^{\circ}\text{C}}$, MPa	131	119	116	198	170
ϵ , %	8	12	6	8	6

Taking into account the phase-rule diagrams it is possible to argue that all the alloying elements which make up the sample, contribute to an increase in hardness with the mass fraction content increasing of each alloying elements by both solid solution hardening and excessive formation of nanoscale phases.

After hot deformation rate and hardness correlation of different alloys vary in accordance with the proceeding structural and phase transformations.

4. Conclusions. By adjusting the alloy composition and thermomechanical treatment modes it is possible to form triplex structure ($\gamma - \alpha - \text{k-carbide}$; $\gamma - \epsilon - \text{k-carbide}$; $\gamma - \epsilon - \alpha$) with different correlation, sizes and phase distribution, providing a given set of mechanical and physical properties.

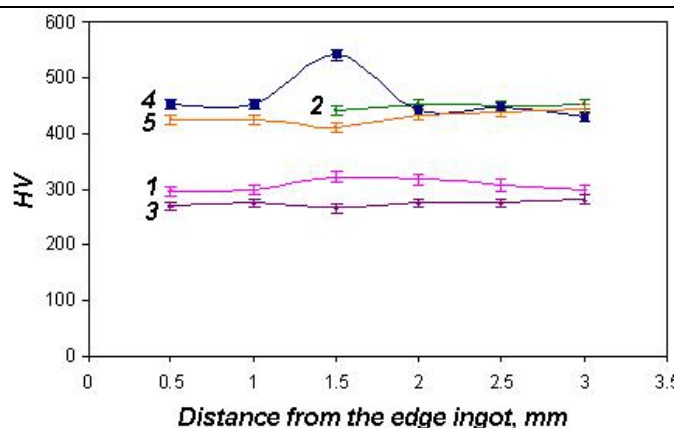


Figure 6 – The alloys hardness after hot deformation. $T=1000\text{ }^{\circ}\text{C}$, $\dot{\epsilon}=0,1\text{ s}^{-1}$.

The addition of nitrogen reduces the melt separation, stabilizes the austenite, lowers the martensitic transformation temperature, and therefore reduces the ϵ -martensite amount formed during cooling.

Hardness at room temperature in the cast state is higher, when the degree of alloy doping is higher. High-carbon alloys with 7.5 and 9% Al have maximum hardness. An alloy with 9% Al has a greater tendency to dendritic segregation and graphitisation, alloys 2 and 5 (4,0 – 6,2% Al) have the greatest inhomogeneity. After hot deformation rate and correlation hardness of different alloys vary as a result of additional occurring structural and phase transformations.

5. References.

- Grassel O., Kruger L., Frommeyer G., Meyer L.W. High strength Fe-Mn-(Al,Si) TRIP/TWIP steels development – properties – application // International Journal of Plasticity. 2000, №16, P. 1391-1409.
- Frommeyer G., Brux U. Microstructures and Mechanical Properties of High-Strength Fe-Mn-Al-C Light-Weight TRIPLEX Steels // Steel Research International. 2006. 77. № 9-10. P. 627-633.
- Bogachev I.N., Egolaev V.F. The structure and properties of iron-manganese alloys. Moscow: Metallurgy, 1973. – p. 295.
- Volynova T.F. High-manganese steels and alloys. Moscow: Metallurgy, 1988. – p. 343.
- Mazanecova E., Jonsta Z., Mazanec K. Structural Metallurgy Properties of high manganese Fe-Mn-Al-C alloy // METALL 2008, Hradec nad Moravici, May 13 – 15.
- Krivanogov G.S., Alekseenko M.F., Solov'eva G.G. The kinetics of phase transformations in 9G28Yu9MVB steel // Phys. Met. and Metall. 1975, № 39, p. 86 – 92.
- Storchak N.A., Drachinskaya A.G. Nature of the work-hardening Fe-Mn-Al-C alloys during aging // Phys. Met. and Metall. 1977, № 44, p. 123 – 130.
- Han K.H., Kang T.S. and Laughlin D.E. Thermomechanical Treatment of an Fe-Mn-Al-C Sideband Alloy // Proc. of International Conference with 1988 World Materials Congress, Chicago, IL. 1988, Sept. 24-30, p. 69-75.
- Prokoshkina V.G., Kaputkina L.M., Svyazhin A.G. The investigation of cast and thermomechanically hardened nitrogen-containing chromium-nickel steel // Metall Tech. and Treatment of Met. 2000. № 9. p. 10-15.
- Kaputkina L.M., Prokoshkina V.G. The features of transformations, the structure and hardening of nitrogen-containing steels // Phase and structural transformations in steels: coll. scien. works. / Edit. by V.N. Urtsev. Magnitogorsk. 2008. №.5, p.138-156.
- Kostina M.V., Bannych O.A., Blinov V.M. The features of steels alloyed with nitrogen // Metall Tech. and Treatment of Met. 2000. № 12. p. 3-6.